http://dx.doi.org/10.11142/jicems.2013.2.4.429
Journal of International Conference on Electrical Machines and Systems Vol. 2, No. 4, pp. 429~435, 2013

Sensorless Control for Surface Mounted Permanent Magnet Synchronous Machines at Low Speed

Lu An *, David Franck *, and Kay Hameyer *

Abstract – This paper proposes a sensorless speed control based on a novel extension of the torque producing flux (active flux) observer for the surface mounted permanent magnet synchronous machines (SPMSM) without additional high frequency signal injection. From the estimated torque producing flux, the rotor position and speed can be calculated at low speed due to their independency. Therefore, no rotor position sensor is required. Two approaches of the torque producing flux observer are presented and compared. The results show the stability and robustness of the expansion of the torque producing flux observer at low speed for the SPMSM.

Keywords: **Low speed, Sensorless control, Surface mounted magnet, PMSM**

1. Introduction

Sensorless control for electrical machines plays an important role in industry applications, in which the number of hardware components and system costs can be significantly reduced. Besides, low installation space requirement and less electromagnetic compatibility problems are also advantages of the sensorless control principles.

There are two categories of sensorless control for the surface mounted permanent magnet synchronous machines, which are used in two different speed ranges, i.e. high speed range and low speed range.

In [1]-[4], the high frequency signal injection method is used in order to diagnose the magnetic saliency, which contains the information about the rotor position and rotor speed. It is one of the most used methods, which are appropriate for low speeds.

In [5], the rotor position is obtained from a predefined ramp function of the rotor speed. The rotor position can be determined through the integral of the rotor speed. This approach for low speed is switched to the one for high speed range, after the rotor ramps up with a constant q-current along this predefined ramp from standstill to a fixed high speed range.

A similar method is used in [6], where a I-f feedforward control is realised at low speed for rotor position and rotor speed estimation. In relation to [5], a reference frequency of stator current is predefined. The stator currents $i_d = 0$ and iq=constant are operated separately. With the aid of the reference frequency, the reference rotor position can be detected.

In addition, the non-linearity of stator inductance can be utilized for the rotor position estimation [7]-[8]. Here, the self-inductance and mutual-inductance are considered. These are dependent on the rotor position. The difference between the stator voltages in free-wheeling mode operation and in converter-active-operation is determined. The information about the rotor position can be detected from this difference.

"Back EMF" method is usually used for the rotor position and rotor speed estimation. Matsui's observer is an extension of the "back EMF" observer [9]. Two redundant parameter models are established: an electrical parameter model and a mechanical parameter model, which contain the information about the rotor position and the rotor speed. An optimal experimental approach is required, in order to provide the extended "back EMF" method for the rotor position and rotor speed estimation at low speed.

In literature, a torque producing flux concept [10]-[11] provides the speed estimation at low speed without the common approach of signal injection. Such methods are suitable for interior permanent magnet synchronous motor (IPMSM). This paper introduces an extension for SPMSM, which is based on the torque producing flux method and combines a disturbance feedforward. The extension model is integrated into the observer model and is inside the

* Institute of Electrical Machines, RWTH Aachen University, Schinkelstr. 4, 52062 Aachen Germany (Lu.An@iem.rwth-aachen.de, david.franck@iem.rwth-aachen.de, Kay.Hameyer@iem.rwth-aachen.de)
Received 3 November 2013; Accepted 29 November 2013

feedback circuit of the observer. Thereby, the uncertainty of the machine parameters and the measurement inaccuracy are considered in order to improve the estimation results. The advantage of the presented approach is the low computational cost. The paper is organized as follows: Section 2: Sensorless Speed Control, Section 3: Observer model, Section 4: Experiment, Section 5: Conclusion.

2. Sensorless Speed Control

In this paper, a cascade control is used for sensorless speed control. Fig. 1 shows that the cascade control consists of speed control circle and current control circle, which are linked with each other. The current controller is the inner loop controller and the speed controller is the outer loop controller. The speed controller output i_q^* is used as the reference variable for the i_q current controller.

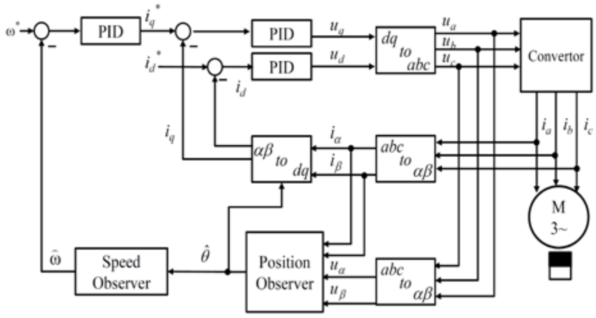

Fig. 1. Sensorless speed control scheme.

Due to the linear independence of the stator currents in *dq* coordinates, it is possible to control the two current components i_d and i_q separately. The direct axis current i_d is set to zero in order to control the torque produced by quadrature axis current i_q. Only the q-component is responsible for the construction of a torque control so that the current control of q-component can superimpose the speed control. Thereby, the PID controller is implemented in the control system.

The stator currents i_q, i_d and the rotor speed are controlled separately. The differential equation of a ideal PID controller in parallel structure:

$$u(t) = K_p \cdot \left[e(t) + \frac{1}{T_{reset}} \int_0^t e(\tau) d\tau + T_{rate} \frac{d}{dt} e(t) \right], \qquad (1)$$

where K_p is the proportional gain, T_{rate} is the rate time and the reset time is T_{reset}. The PID controller can also be described as transfer function:

$$\frac{U(s)}{E(s)} = K_p \cdot \left[1 + \frac{1}{T_{reset} + s} + T_{rate} \cdot s \right]. \qquad (2)$$

The controller parameters of the PID controllers for the current and speed control are listed in Table 1.

Table 1. Parameters of PID Controllers

Controlled variable	Controller parameters
Stator current (quadrature axis) i_q	Proportional gain $K_{p,iq}$
	Rate time $T_{rate,iq}$
	reset time $T_{reset,iq}$
Stator current (direct axis) i_d	Proportional gain $K_{p,id}$
	Rate time $T_{rate,id}$
	reset time $T_{reset,id}$
Rotor Speed ω	Proportional gain $K_{p,\omega}$
	Rate time $T_{rate,\omega}$
	Reset time $T_{reset,\omega}$

An exact rotor position is required to control the PMSMs. Therefore, a sensorless control with position observer is designed to provide exact rotor position. A complete block diagram representation for a sensorless control of PMSM using a voltage regulated space vector PWM voltage source inverter is shown in Fig. 1. The observers estimate the rotor position and speed using the stator currents i_s^s and voltage u_s^s in the $\alpha\beta$ coordinate system, which are calculated from the measured stator currents $i_{a,b,c}$ and voltages $u_{a,b,c}$. The estimated rotor position is used for the Park's transformation and the estimated speed is fed back to the speed control.

3. Observer Models

3.1 Observer Model with Flux Feedback

The principle of the torque producing flux observer with flux feedback is shown in Fig. 2 [10]: the aim of this method is an accurate estimation of the torque producing flux (active flux).

With the help of the voltage model (3) [10], the estimated stator flux $\hat{\Psi}_s^s$ can be calculated from the current i_s^s and voltage u_s^s :

$$u_s^s = R_s i_s^s + d\Psi_s^s / dt. \qquad (3)$$

R_s is the stator resistance. $i_s^s = (i_\alpha, i_\beta)^T$ and $u_s^s = (u_\alpha, u_\beta)$ are stator current und voltage in $\alpha\beta$-coordinates, which are calculated from measured 3 phases stator current $i_{a,b,c}$ und

3 phases stator voltage $u_{a,b,c}$. The current model [10]

$$\hat{\Psi}_{si}^{r} = \Psi_{si,d} + j\Psi_{si,q} = \begin{pmatrix} \Psi_F \\ 0 \end{pmatrix} + \begin{pmatrix} L_d & 0 \\ 0 & L_q \end{pmatrix} \begin{pmatrix} i_d \\ i_q \end{pmatrix} \quad (4)$$

is defined to estimate the magnetic flux $\hat{\Psi}_{si}^{r}$, which is in dq-coordinates and has to be transformed in $\alpha\beta$-coordinates:

$$\hat{\Psi}_{si}^{s} = T^{-1}(\theta)\cdot\hat{\Psi}_{si}^{r}\,. \quad (5)$$

The transformation matrix from dq to $\alpha\beta$ is described as

$$T^{-1}(\theta) = \begin{pmatrix} \cos(\theta) & -\sin(\theta) \\ \sin(\theta) & \cos(\theta) \end{pmatrix}. \quad (6)$$

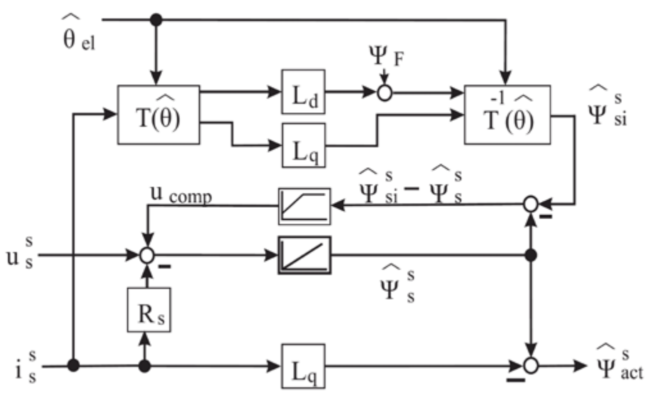

Fig. 2. Structure of the torque producing flux observer with flux feedback.

As shown in Fig. 2, the difference between the estimated $\hat{\Psi}_{s}^{s}$ and $\hat{\Psi}_{si}^{s}$ is fed back to the voltage model through the PI compensator gain. Thereby, the estimation of the stator flux can be corrected and improved:

$$\hat{\Psi}_{s}^{s} = \int \left(u_s^s - R_s i_s^s + u_{comp}\right) dt\,. \quad (7)$$

The compensation value u_{comp} in s-domain is described as:

$$u_{comp} = \left(k_p + k_i/s\right)\cdot\left(\hat{\Psi}_{si}^{s}(s) - \hat{\Psi}_{s}^{s}(s)\right), \quad (8)$$

where k_p is the proportional gain and k_i is integral gain, which can be experimentally ascertained.

In order to get closer insight into the characteristics of the permanent flux in $\alpha\beta$-coordinates, the active flux is defined as [10]:

$$\hat{\Psi}_{act}^{s} = \hat{\Psi}_{s}^{s} - L_q i_s^s \quad (9)$$

where L_q is the q-axis stator self inductance and Ψ_F is the stator flux. The rotor position $\hat{\theta}_{el}$ can be estimated by

$$\hat{\theta}_{el} = \arccos\left(\hat{\Psi}_{act,\alpha} \Big/ \sqrt{\hat{\Psi}^2_{act,\alpha} + \hat{\Psi}^2_{act,\beta}}\right) + n\cdot\pi\,, \quad (10)$$

with $n = N_0$. The rotor position $\hat{\theta}_{el}$ can also be calculated by arctangent function of $\hat{\Psi}_{act,\beta} / \hat{\Psi}_{act,\alpha}$.

3.2 Observer Model with Current Feedback

The principle of the observer with current feedback is shown in Fig. 3: similar to the flux observer with flux feedback, this observer model consists of a current model (11) and a voltage model (12) [11]:

$$\begin{pmatrix} \hat{i}_\alpha \\ \hat{i}_\beta \end{pmatrix} = T^{-1}(\hat{\theta})\cdot\begin{pmatrix} 1/L_d & 0 \\ 0 & 1/L_q \end{pmatrix}\cdot T(\hat{\theta})\cdot\begin{pmatrix} \hat{\Psi}_\alpha \\ \hat{\Psi}_\beta \end{pmatrix} + \frac{\Psi_F}{L_d}\cdot\begin{pmatrix} \cos(\hat{\theta}) \\ -\sin(\hat{\theta}) \end{pmatrix}; \quad (11)$$

$$\frac{d}{dt}\begin{pmatrix} \hat{\Psi}_\alpha \\ \hat{\Psi}_\beta \end{pmatrix} = -R_s\cdot\begin{pmatrix} i_\alpha \\ i_\beta \end{pmatrix} + \begin{pmatrix} u_\alpha \\ u_\beta \end{pmatrix} + K\cdot\begin{pmatrix} i_\alpha - \hat{i}_\alpha \\ i_\beta - \hat{i}_\beta \end{pmatrix}. \quad (12)$$

$\hat{\Psi}_\alpha$ and $\hat{\Psi}_\beta$ are estimated stator flux quantities in $\alpha\beta$-coordinates and used to determine the present stator current. Through the proportional control factor K, the difference between the estimated stator current $\hat{i}_s^s = \left(\hat{i}_\alpha, \hat{i}_\beta\right)^T$ and the measured stator current $i_s^s=(i_\alpha, I_\beta)^T$ is the feed-back signal of the voltage model to be minimized. The active flux $\hat{\Psi}_{act}^{s}$ is determined by (9). The rotor speed can be defined with estimated rotor position $\hat{\theta}_{el}$ (10) as

$$\hat{\omega}_{mech} = \dot{\hat{\theta}}_{mech} = \frac{d\hat{\theta}_{mech}}{dt} = \frac{d}{dt}\frac{\hat{\theta}_{el}}{p} \quad (13)$$

or with an equation as a function, that depends on the difference between the previous and the current values of the estimated active flux:

$$\omega_{mech} = \left(\theta_{mech,n} - \theta_{mech,n-1}\right)/T, \quad (14)$$

$$\omega_{mech} = \frac{1}{T}\cdot\frac{1}{p}\cdot\left[\arctan\left(\frac{\Psi_{act,\beta_n}}{\Psi_{act,\alpha_n}}\right) - \arctan\left(\frac{\Psi_{act,\beta_{n-1}}}{\Psi_{act,\alpha_{n-1}}}\right)\right], \quad (15)$$

where p is number of pole pairs and T is the sampling time.

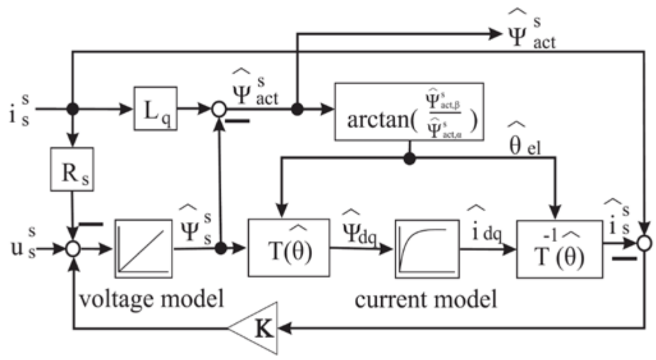

Fig. 3. Structure of the torque producing flux observer with current feedback.

3.3 Stability Analysis

The stability of the observer model has already been stated in [12]. The estimated errors can be described as

$$i_{s,e}^{s} = -C \cdot \Psi_{s,e}^{s} \tag{16}$$

with

$$C = T^{-1}(\hat{\theta}) \begin{pmatrix} \frac{1}{L_d} & 0 \\ 0 & \frac{1}{L_q} \end{pmatrix} T(\hat{\theta}). \tag{17}$$

The dynamics of the state errors can be defined by

$$\frac{d}{dt}\Psi_{s,e}^{s} = -K \cdot i_{s,e}^{s} = -KC \cdot \Psi_{s,e}^{s}. \tag{18}$$

A Lyapunov candidate function of the observer model is given by

$$V = \frac{1}{2}\Psi_{s,e}^{s\ T}\Psi_{s,e}^{s} > 0. \tag{19}$$

The derivative of the Lyapunov candidate function is defined as

$$\dot{V} = \frac{d}{dt}V = \Psi_{s,e}^{s\ T}\frac{d}{dt}\Psi_{s,e}^{s} = -\Psi_{s,e}^{s\ T}KC\Psi_{s,e}^{s}. \tag{20}$$

The model of the observer is asymptotically stable, because $\dot{V}$ is smaller than zero with all of the positive eigenvalues of the function KC.

3.4 Extension of Observer Model

In order to be able to improve the estimation results, an extension of the observer is developed. Thereby, the uncertainty of the machine parameters is considered, e.g.: the non-linearity of the stator inductance $L+\underset{\sim}{L}$ and the change of resistance with temperature $R+\underset{\sim}{R}$. Furthermore, the measurement accuracy could also affect the estimation results. The above-mentioned variables are defined as the disturbance variable of the observer system. The additional estimation errors are caused by the disturbance variables.

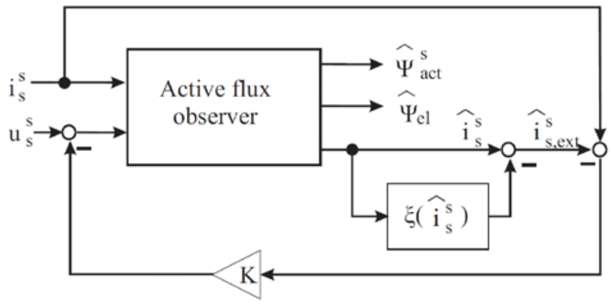

Fig. 4. Extension of observer model.

Fig. 4 describes the principle of the extension. At this, the estimated current $\hat{i}_s^s = (\hat{i}_\alpha, \hat{i}_\beta)^T$ is selected as the input variable of the extension. Afterwards, the estimated current $\hat{i}_s^s$ is corrected to $\hat{i}_{s,ext}^s$. The extension model is a part of the observer model and is inside the feedback circuit of the observer. Through the proportional control factor K, the difference between the measured stator current i_s^s and the extended estimated stator current $\hat{i}_{s,ext}^s$ which is corrected by the extension is the feed-back signal to be minimized. With the help of experiments, the correlation between the estimated current und the disturbance variable ξ can be simplified to

$$\xi(x) = k_1 x^2 + k_2 x \quad . \tag{21}$$

The parameter k_1 and k_2 can be ascertained from the measurement.

4. Experiment

4.1 Test Bench

The parameters of the SPMSM used in the simulation and experiment are collected in Tab. 2. In contrast to the interior permanent magnet synchronous motor (IPMSM), the stator inductance of the quadrature axis and direct axis (L_q and L_d) of SPMSM has the same values. The above presented methods were implemented for the SPMSM.

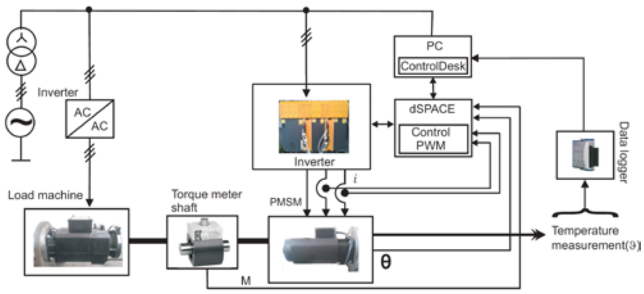

Fig. 5. Experimental test platform.

The experimental system setup and testing setup with hardware components are defined as in Fig. 5. The above depicted sensorless control method is implemented to a dSPACE platform for the permanent magnet synchronous machines. Thereby, a three-phase asynchronous machine (ASM) is utilised as a load machine, which is controlled by an inverter in order to provide the desired torque. The PWM frequency of the inverter is 8 kHz. The dSPACE CLP1103 is used to control the drive system (Fig.5).

The stator currents and voltages are measured and the sampling rate is 20 kHz. The information are transmitted to the dSPACE platform. A torque gauge bar is installed on the shaft between the asynchronous machine and the PM machine for the torque measure.

The estimated rotor position is sent to the Control Desk. The return of the Control Desk is fed back to the dSPACE system. The inverter inherits the approval and the suitable signals, which are the inputs of the PM machine.

4.2 Estimation and Control Results

The estimation result of the current by using flux observer with current feedback without compensation at the speed of 30 rpm is shown in Fig. 6, where the measured current is plotted. It can be seen that the shape of the estimated current is similar to the measured current. However, its peak value does not accord with the peak value of the measured current i_s^s.

This deviation cannot be rectified by the adjustment of the proportional control factor *K* (Fig. 3). The reason for this is that the estimated current and measured current i_s^s are coupled by the control factor *K*, the voltage model and the current model.

Furthermore, the inaccurate parameters of the PMSM have negative impact on the estimated current and the estimated rotor position, which influence each other. It is intricate to minimize the estimation error only by changing the control factor *K*.

Fig. 7 illustrates the current estimation result by using compensation (Fig. 4), which does not strongly depend on the motor parameters variation. The negative impacts on the estimation are considered, e.g. the stator resistance change due to the motor temperature rise and influence of inductance variation. The estimation error is considerably minimized.

An incremental encoder was used to measure the rotor position which was considered as reference. The estimated rotor position and the measured rotor position are shown in Fig. 8. By comparison, although having a tiny time delay around 20 ms to the measured rotor position.

The results of the developed sensorless speed control are shown in Fig. 9. The dead-time is 10 ms. Both of the approaches are stable at low speed. However, the controller with "flux feedback" results in overshoots and is even instable at the speed of 5 rpm. When compared to "flux feedback", the "current feedback" shows improved stability and performance at low speed.

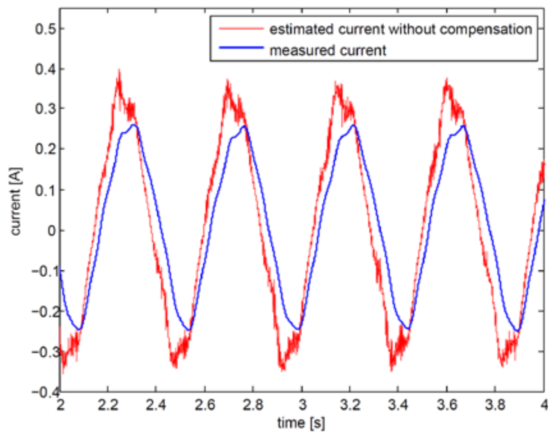

Fig. 6. Estimated current without compensation.

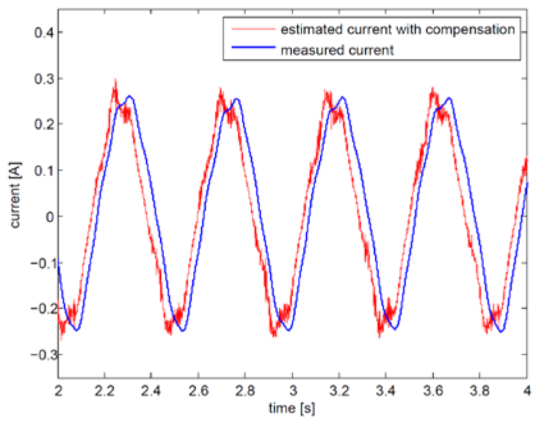

Fig. 7. Estimated current with compensation.

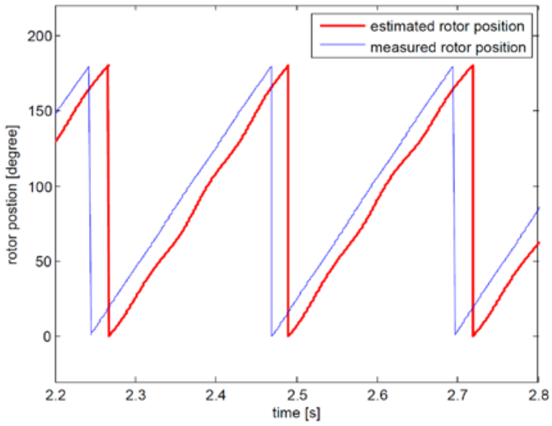

Fig. 8. Rotor position estimation.

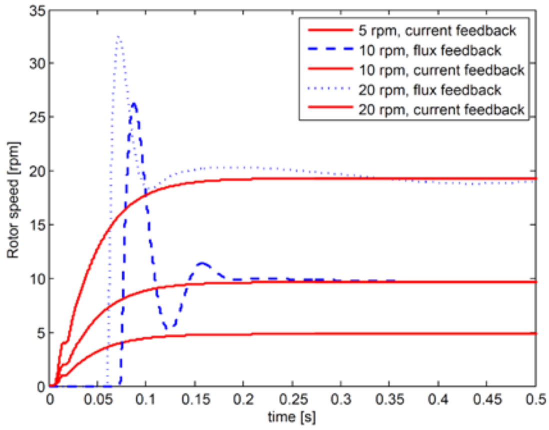

Fig. 9. Comparison of two approaches.

The observer with "current feedback" provides better results in comparison to the one with "flux feedback". The reason behind is, that the flux $\hat{\Psi}_s^s$ (Fig. 2) is not directly measured by the "flux feedback" and it is calculated from the measured stator currents und voltages.

Because of this additional conversion, the values of flux $\hat{\Psi}_s^s$ could actually differ from the real value. By "current feedback", the estimated current is compared to the measured current without further transformation (Fig. 3). This leads to less overlay error.

5. Conclusions

In this paper two torque producing flux (active flux) observer models for sensorless speed control of the surface mounted permanent magnet synchronous machines are presented and compared to each other.

An extension of the observer is developed in order to improve the estimation procedure. Thereby, the uncertainty of the machine parameters is considered und the error of the current estimation is minimized. Therefore, the exact active flux can be determined.

By the control using observers, the observer model with current feedback provides better result in comparison to the observer model with flux feedback and shows improved stability and performance at low speed.

Appendix

Table 2. Specifications of PMSM

Parameters and constraints	Value
Number of pole pairs p	4
Maximum speed n_{max}	4500 [rpm]
Rated speed n_N	2000 [rpm]
Rated power P_N	10.3 [kW]
Rated phase to phase voltage U_N	380 [V]
Maximum permitted motor current I_{max}	75 [A]
Rated motor current I_N	21.2 [A]
Rated torque T_N	49.2 [Nm]
Mass moment of inertia J	$60{\cdot}10^{-3}$ [kg·m2]
Stator resistance R_s	0.2 [Ω]
Stator inductance (quadrature axis) L_q	0.005 [H]
Stator inductance (direct axis) L_d	0.005 [H]
Excitation flux ψ_F	0.2735 [Vs]
Time constant (quadrature axis) $t_q = L_q/R$	0.025 [H/ Ω]
Time constant (direct axis) $t_d = L_d/R$	0.025 [H/ Ω]
Coefficient of friction µ	0

References

[1] Jung-Ik Ha; Ide, K. Sawa, T., and Seung-Ki Sul, "Sensorless rotor position estimation of an interior permanent-magnet motor from initial states," *IEEE Transactions on Industry Applications*, vol. 39, pp 761 - 767, May 2003.

[2] Ji-Hoon Jang, Seung-Ki Sul, Jung-Ik Ha, abd Ide, K., "Sensorless drive of surface-mounted permanent-magnet motor by high-frequency signal injection based on magnetic saliency," *IEEE Transactions on Industry Applications*, vol. 39, pp 1031 - 1039, July 2003.

[3] Dan Xiao, Foo, G., Rahman, M.F., "Sensorless direct torque and flux control for matrix converter IPM synchronous motor drives using adaptive sliding mode observer combined with high frequency signal injection," *IEEE Transactions on Energy Conversion Congress and Exposition, ECCE* , pp 4000 - 4007, September 2009.

[4] Piippo, A., and Luomi, J., "Sensorless adaptive observer combined with HF signal injection for sensorless control of PMSM drives," *Electric Machines and Drives*, pp 674 - 681, May 2005.

[5] Zihui Wang, Kaiyuan Lu, Blaabjerg, F., "A simple startup strategy based on current regulation for back-EMF-based sensorless control of PMSM," *Power Electronics*, vol. 27, pp 3817 - 3825, August 2012.

[6] Fatu, M., Teodorescu, R., Boldea, I., Andreescu, G., and Blaabjerg, F., "I-F starting method with smooth transition to EMF based motion-sensorless vector control of PM synchronous motor/generator," *Power Electronics Specialists Conference, 2008. PESC 2008. IEEE*, pp 1481 - 1487, June 2008.

[7] Cheng-Kai Lin, Tian-Hua Liu, and Chi-Hsun Lo, "High performance sensorless IPMSM drive with a wide adjustable speed range," *Industrial Electronics, 2008. IECON 2008. 34th Annual Conference of IEEE*, pp 1222 - 1227, November 2008.

[8] Lin, C.-K., Liu, T.-H., Lo, and C.-H., "Sensorless interior permanent magnet synchronous motor drive system with a wide adjustable speed range," *Electric Power Applications, IET*, vol. 3, pp 133 - 146, March 2009.

[9] Caux, S., and Maussion, P., "Optimal setting of PMSM observer parameters using 2D experimental designs," *Power Electronics, Electrical Drives, Automation and Motion, 2008. SPEEDAM 2008. International Symposium*,pp 8 - 13, June 2008.

[10] B. Ion, P. Mihaela Codruta, A. Gheorghe-Daniel, and B. Fre, "Active flux" DTFC-SVM sensorless control of IPMSM," *IEEE Transactions on Energy Conversion*, vol. 24, no. 2, pp. 314-322, JUNE 2009.

[11] F. Gilbert Hock Beng, and M. F. Rahman, "Direct torque control of an IPM-synchronous motor drive at very low speed using a sliding-Mode stator flux observer," *IEEE Transactions on Power Electronics*, vol. 25, no. 4, pp. 933-942, April 2010.

[12] Foo, G., Rahman, M.F., "Sensorless vector control of interior permanent magnet synchronous motor drives at very low speed without signal injection," *Electric Power Applications, IET,* vol. 4 , no. 3, pp. 131 -139, 2010.

Lu An was born in Liaoning, China. She received the Dipl.-Ing. degree in electrical engineering from Gottfried Wilhelm Leibniz University Hannover, Hannover, Germany. She has been working as a research associate at the Institute of Electrical Machines of RWTH Aachen University, Germany since October 2009.

Her research interests include sensorless control of permanent magnet synchronous machines.

David Franck received his diploma in Electrical Engineering in 2008 as Engineer from the Faculty of Electrical Engineering and Information Technology at RWTH Aachen University. Since, 2008 he has worked as a researcher at the Institute of Electrical Machines (IEM) at RWTH Aachen University.

He is currently working towards his doctoral degree in the area of noise and vibration of electrical machine

Kay Hameyer (FIET, SMIEEE) received his M.Sc. degree in electrical engineering from the University of Hannover and his Ph.D. degree from the Berlin University of Technology, Germany.

After his university studies he worked with the Robert Bosch GmbH in Stuttgart, Germany as a Design Engineer for permanent magnet servo motors and vehicle board net components.

Until 2004 Dr. Hameyer was a full Professor for Numerical Field Computations and Electrical Machines with the KU Leuven in Belgium.

Since 2004, he is full professor and the director of the Institute of Electrical Machines (IEM) at RWTH Aachen University in Germany. 2006 he was vice dean of the faculty and from 2007 to 2009 he was the dean of the faculty of Electrical Engineering and Information Technology of RWTH Aachen University. His research interests are numerical field computation and optimisation, the design and controls of electrical machines, in particular permanent magnet excited machines, induction machines and the design employing the methodology of virtual reality. Since several years Dr. Hameyer's work is concerned with the development of magnetic levitation for drive systems, magnetically excited audible noise in electrical machines and the characterisation of ferro-magnetic materials.

Dr. Hameyer is author of more then 250 journal publications, more then 500 international conference publications and author of 4 books. Dr. Hameyer is a member of VDE, IEEE senior member, fellow of the IET.